Available online at www.sciencedirect.com
SCIENCE DIRECT
Journal of Photochemistry and Photobiology A: Chemistry 178 (2006) 76–82
Journal of Photochemistry and Photobiology A:Chemistry
www.elsevier.com/locate/jphotochem

Intramolecular proton transfer in 4-methyl-2,6-diformyl phenol and its derivative studied by femtosecond transient absorption spectroscopy

S. Mitra [a,*], N. Tamai [b], S. Mukherjee [c]

[a] *Department of Chemistry, North-Eastern Hill University, Permanent Campus, Umshing, Shillong, Meghalaya 793022, India*
[b] *Department of Chemistry, School of Science & Technology, Kwansei Gakuin University, 2-1 Gaku-en, Sanda, Hyogo 669 1337, Japan*
[c] *Department of Physical Chemistry, Indian Association for the Cultivation of Science, Jadavpur, Calcutta 700032, India*

Received 6 April 2005; received in revised form 31 May 2005; accepted 6 July 2005
Available online 3 August 2005

Abstract

Dynamics of excited state intramolecular proton transfer (ESIPT) and solution phase fluorescence properties of 4-methyl-2,6-diformyl phenol (MFOH) and its derivative, 4-methyl-2,6-diacetyl phenol (MAOH), have been monitored by nanosecond time correlated single photon counting and femtosecond transient absorption techniques. Time evolution of the transient absorption data reveals that both the compounds undergo an ultrafast proton transfer, yet with a significantly slower rate constant of about $4–5 \times 10^{12}\ s^{-1}$ compared to the other intramolecularly hydrogen bonded systems reported recently. This is explained on the basis of large skeletal rearrangement necessary for the proton transfer to occur. The ultrafast ESIPT process is followed by rapid intramolecular vibrational relaxation (IVR) with a time constant of few picoseconds before fluorescence emission occurs from the proton transferred keto structure in the excited state potential energy surface.

Keywords: ESIPT; Femtosecond transient absorption; IVR; Fluorescence spectroscopy

1. Introduction

Proton transfer reactions play a central role in a number of chemical and biological processes [1–5]. Molecules undergoing excited state intramolecular proton transfer (ESIPT) are also proposed to have several technological importance like ultraviolet (UV) stabilizer [6], sources for tunable lasers [7], for information storage and optical switching [8], etc. Moreover, ESIPT reactions can be used efficiently as a probe to study the binding sites and conformations of proteins [9–10] and also to explore the hydrophobic nanocavities like cyclodextrins [11–12].

The primary feature common to the most ESIPT systems is the extreme rapid rate of proton transfer through a pre-existing strong intramolecular hydrogen bond under excitation in the gas phase as well as in non-polar solvents where environmental perturbation is negligible. For molecules with relatively weak intramolecular hydrogen bond, perturbation from polar especially protic environments may modify the ESIPT dynamics, which may either be prohibited within the excited-state life span or proceed with a prerequisite of (protic) solvent reorganization. The number and nature of the resulting conformers differ with the individual system under consideration depending on its hydrogen bonding strength and other physical properties of the solvent medium. However, the basic picture remains the same, i.e., the proton (or more strictly, hydrogen) moves very fast (within the range from pico to femtosecond time scale) from the donor to the acceptor atom in a six (or five) membered hydrogen bonded system [13–14] due to the complete reversal of pK_a in the excited state compared to the ground state. A number of recent ultrafast laser experiments with diverse techniques have been reported on ESIPT that gives direct access to experimental measurement of the proton transfer rates [15–17].

The majority of ESIPT rates those have been determined involve the systems where nitrogen acts as proton acceptor. The examples include the ESIPT time of 160 ± 20 fs for 2-

* Corresponding author. Tel.: +91 364 272 2634; fax: +91 364 255 0486.
E-mail address: smitra@nehu.ac.in (S. Mitra).

1010-6030/$ – see front matter © 2005 Elsevier B.V. All rights reserved.
doi:10.1016/j.jphotochem.2005.07.002

(2′-hydroxy phyenyl) benzothiazole (HBT) in dichloroethane [18], ∼100 fs for 2-(2′-hydroxy, 5′-methyl phenyl) benzotriazole in non-polar solvents [19] and less than 300 fs for [2,2′-bipyridyl] 3,3′-diol [20]. More recent experiments by Neuwahl et al. [21] reported less than 50 fs limit of the ESIPT of [2,2′-bipyridyl] 3,3′-diol. Recent results with 30 fs time resolution pump probe spectroscopy on the proton transfer of HBT in cyclohexane reveals that about 33 fs after the excitation the molecule adopts a keto configuration and about 20 fs later, the potential minimum of the keto form is achieved [22]. Ernsting et al. [23] reported 110 ± 15 fs time constant for the conversion of enol form of 2,5-bis (2′-benzoxazolyl) hydroquinone to the corresponding keto form in tetrahydrofuran. Femtosecond dynamics of double proton transfer in 7-azaindole dimer has also been reported by several groups [24–26] and found to occur within few hundreds of femtoseconds.

Measurement of ESIPT rates for the systems involving oxygen as proton donor and acceptor are relatively less. Femtosecond fluorescence depletion studies on methyl salicylate (MS) report 60 ± 10 fs for the proton transfer [27]. Ernsting and Dick [28] calculated ESIPT rate constant from the line shape of jet cooled emission of 3-hydroxyflavone (3-HF) as $7.4 \times 10^{11}\ s^{-1}$. However, recent ultrafast pump-probe studies on the dynamics of 3-HF reveal ESIPT time of 35 fs in methyl cyclohexane and acetonitrile, whereas 60 fs time constant has been reported in ethanol [29].

The six membered intramolecularly hydrogen bonded systems 4-methyl-2,6-diformyl phenol (MFOH, **I**) and its derivative, 4-methyl-2,6-diacetyl phenol (MAOH, **II**) are prototype examples (Fig. 1, for structures) showing ESIPT phenomena [30,31]. However, no report on the dynamics of proton transfer for these systems is available. Measurement of ESIPT dynamics will unravel the mechanism of this fast process in these particular systems as well as the dynamic behavior can be compared with other ESIPT systems. In this present paper, we report the dynamics of solution phase ESIPT and subsequent relaxation process in these systems at room temperature studied by steady state and time resolved fluorescence and also with femtosecond transient absorption spectroscopy.

2. Experimental

Synthesis and purification of 4-methyl-2,6-diformyl phenol (MFOH, **I**) and 4-methyl-2,6-diacetyl phenol (MAOH, **II**) has been described elsewhere [32–33]. The compounds were repeatedly recrystallized from ethanol and dried before use. Spectroscopic grade (99.9+%) cyclohexane and chloroform were received from Aldrich Chemical Co. and used without any further purification.

Steady state absorption and fluorescence spectra of the dilute solution ($\sim 5 \times 10^{-5}$ mol dm^{-3}) of the compounds were recorded in JASCO UV–vis (model 7850) and Perkin-Elmer MPF 44B spectrometers, respectively. Emission spectra were corrected for spectral sensitivity of the instrument. Fluorescence quantum yield (ϕ_F) measurements were performed by comparing the fluorescence intensity, integrated over the whole range of emission frequencies, with that of methyl salicylate ($\phi_F = 0.02$ in cyclohexane) using quinine sulphate as a standard ($\phi_F = 0.51$) [34]. The transient fluorescence lifetimes were measured using time-correlated single photon counting technique with an SP-70 nanosecond spectrometer (Applied Photophysics Ltd.) based on nitrogen flash lamp or using a CW mode-locked Nd:YAG laser system, as described before [30,31].

The details of femtosecond transient absorption set-up were reported elsewhere [35–36]. The laser system consisted of a hybridly mode-locked, dispersion compensated femtosecond dye laser (Coherent, Satori 774) and a dye amplifier (Continuum, RGA 60-10 and PTA 60). The dye laser (gain dye Pyridine 2 and saturable absorber DDI) was pumped with a cw mode-locked Nd:YAG laser (Coherent, Antares 76S). The sample was excited by second harmonic (360 nm) of the fundamental (center wavelength 720 nm) at a repetition rate of 10 Hz. Residual part of the fundamental output was focused

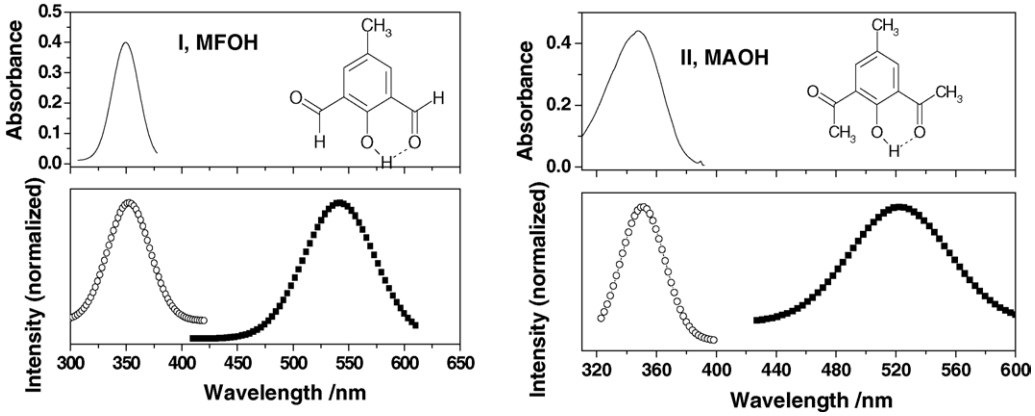

Fig. 1. Steady state absorption (solid line), fluorescence emission (scattered points) and excitation (line + symbol) spectra of MFOH (**I**) and MAOH (**II**) in cyclohexane. The structures of the two compounds are also given in respective panels.

in a 1 cm H_2O cell to generate femtosecond supercontinuum probe pulse. The pump and probe pulses were focused on the sample at magic angle (54.7°) to avoid any anisotropic contribution. A computer controlled translational stage was used to change the time delay between the pump and the probe pulse. Transient spectra were obtained by averaging over 200 pulses and analyzed by an intensified multichannel detector (Princeton Instruments ICCD-576) as a function of probe delay time. The time resolution of the transient absorption measurement system better than 200 fs as discussed before [37]. The temporal resolution of the detection system was checked by the rise and decay of the transient absorption of CS_2 (excitation at 360 nm) that have no rise component and a decay component of few hundreds of femtoseconds. The pulse width was determined in such a way to simulate the dynamic response of CS_2. The spectra were corrected for the intensity variation and time dispersion of the supercontinuum.

Concentration of the samples for transient absorption spectra was kept $\sim 8 \times 10^{-4}$ mol dm^{-3}. A circular variable attenuator was used to reduce the intensity of the pump pulse and also the sample solution were allowed to flow through a 2 mm flow cell using a magnetic gyre pump (Micropump, 040–332) during the transient absorption measurements to avoid any sample damage. It was further confirmed by comparing the steady state absorption profile before and after the transient experiments. Rise and decay curves at a fixed wavelength were measured with a photodiode-monochromator (Japan Spectroscopic, CT-10) combination. The one-wavelength rise and decay curves were analyzed by a non-linear least-square iterative convolution method described previously [35]. All the measurements were carried out at 294 ± 2 K.

3. Results and discussion

3.1. Steady state absorption and emission properties

Steady state absorption and emission properties of MFOH (**I**) and MAOH (**II**) have been measured in both cyclohexane and chloroform at ambient temperature together with their emission quantum yields (ϕ_F). The absorption band maxima for both the compounds are found to be at 350 nm. However, the emission spectra show a large Stokes shifted broad band at 535 nm for **I** and that for **II** at 520 nm. Some representative spectra are shown in Fig. 1. The solvent has almost no effect on the steady state absorption and emission properties for both **I** and **II**. The observed Stokes shift of ~9880 cm^{-1} for **I** and ~9340 cm^{-1} for **II** suggest that the structural geometry of the emissive excited state is significantly displaced from that of the ground state. Based on our previous reports, the 350 nm absorption and the Stokes shifted emission of **I** and **II** could be attributed to enol- (**a**) and proton transferred keto- (**b**) tautomer (Scheme 1), respectively [30,31]. It is to be noted here that the possible formation of other rotamers originated by the torsion of the respective substituted groups, observed previously for *o*-hydroxy benzaldehyde [38,39] and also in the present systems [31], at low temperature matrices in both the cases, are not considered in Scheme 1 as these conformers are not observed spectroscopically at room temperature.

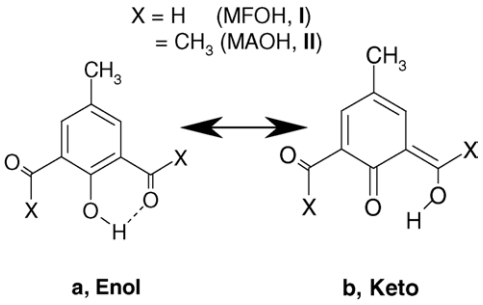

Scheme 1.

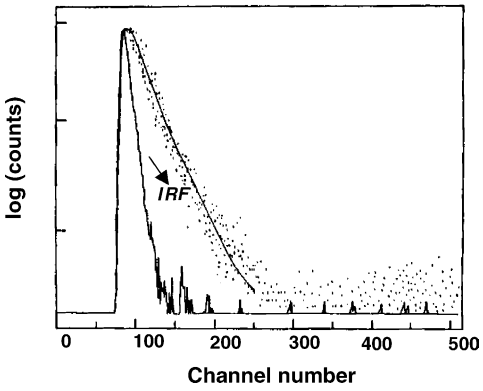

Fig. 2. Typical fluorescence decay profile (dotted points) of **I** in cyclohexane fitted with a single exponential function (solid line). Time resolution = 0.166 ns channel^{-1}. Instrument response function (IRF) is also shown in the figure.

3.2. Nanosecond time resolved fluorescence measurements

The decay profiles of the tautomer emission of **I** and **II** were determined using time correlated single photon counting technique in both the solvents. Fig. 2 shows a typical decay profile of **I** in cyclohexane and Table 1 collects all the decay times. The observed fluorescence decay profiles were convoluted globally using the software provided by Photon Technology International Inc. and found to be single expo-

Table 1
Fluorescence properties of **I** and **II** in different solvents

System	Solvent	ϕ_F	τ_F (ns)	κ_R (10^7 s^{-1})	κ_{NR} (10^8 s^{-1})
MFOH (**I**)	Cyclohexane	0.11	1.2	9.1	7.4
	Chloroform	0.08	1.1	7.3	8.4
MAOH (**II**)	Cyclohexane	0.06	0.9	6.6	10.4
	Chloroform	0.06	0.7	8.6	13.4

nential in all the cases. The goodness of the fit was judged by reduced chi-sqare (χ^2_R) and Durbin–Watson (DW) parameters [40]. Table 1 also shows the rate constants for radiative (κ_R) and non-radiative (κ_{NR}) emission processes calculated using the relations in Eq. (1).

It is observed that the rate constant for the non-radiative processes (κ_{NR}) is about an order of magnitude larger than the rate constants for the radiative processes (κ_R). So, it can be assumed that non-radiative decay process predominates in the deactivation of the excited state of these compounds. It is also interesting to note the higher value of κ_{NR} in

$$\kappa_R = \frac{\phi_F}{\tau_F}; \quad \kappa_{NR} = \frac{(1-\phi_F)}{\tau_F} \tag{1}$$

II compared to **I** in both the solvents. It has been reported previously for similar intramolecularly hydrogen bonded methyl salicylate (MS) that the increase in non-radiative decay rate constant is caused by the large amplitude out-of-plane vibration of the benzene ring including the intramolecular hydrogen bond with the carbonyl group [41,42]. Recent ab-initio calculation result and normal mode analysis on a series of substituted derivative of **I** indeed confirms the above prediction [43].

3.3. Femtosecond transient absorption measurements

Fig. 3 shows the time evolution of transient absorption spectra of $\sim 10^{-4}$ mol dm^{-3} solution of **I** in cyclohexane at different probe time delays after excitation by femtosecond pulse at 360 nm. Both the compounds show similar transient spectral properties in the solvents studied here. The time evolution of transient absorption spectra can be divided in three different regions. Initially, a very broad band appears in the spectral region of 400–560 nm. With time, the shape of the transient absorption spectra is changed and a relatively narrower band in the range of 420–500 nm (with a peak position at about 460 nm) stays even upto the time delay of 500 ps. Moreover, within a time delay of 1 ps between the pump and the probe pulse, a negative absorption appears at ~560 nm. It is also seen that the transient absorption intensity at 460 nm grows upto few picoseconds and then starts decaying in nanosecond time scale.

The initial broad band is believed to be due to the transient absorption of the initially excited enol structure (**a**, Scheme 1) before ESIPT occurs. Recently, we have reported the appearance of broad transient spectra from the initially excited species in similar ESIPT systems like salicyledeneaniline (SA) [36,44] and 2-(2′,4′-dinitrobenzyl)pyridine

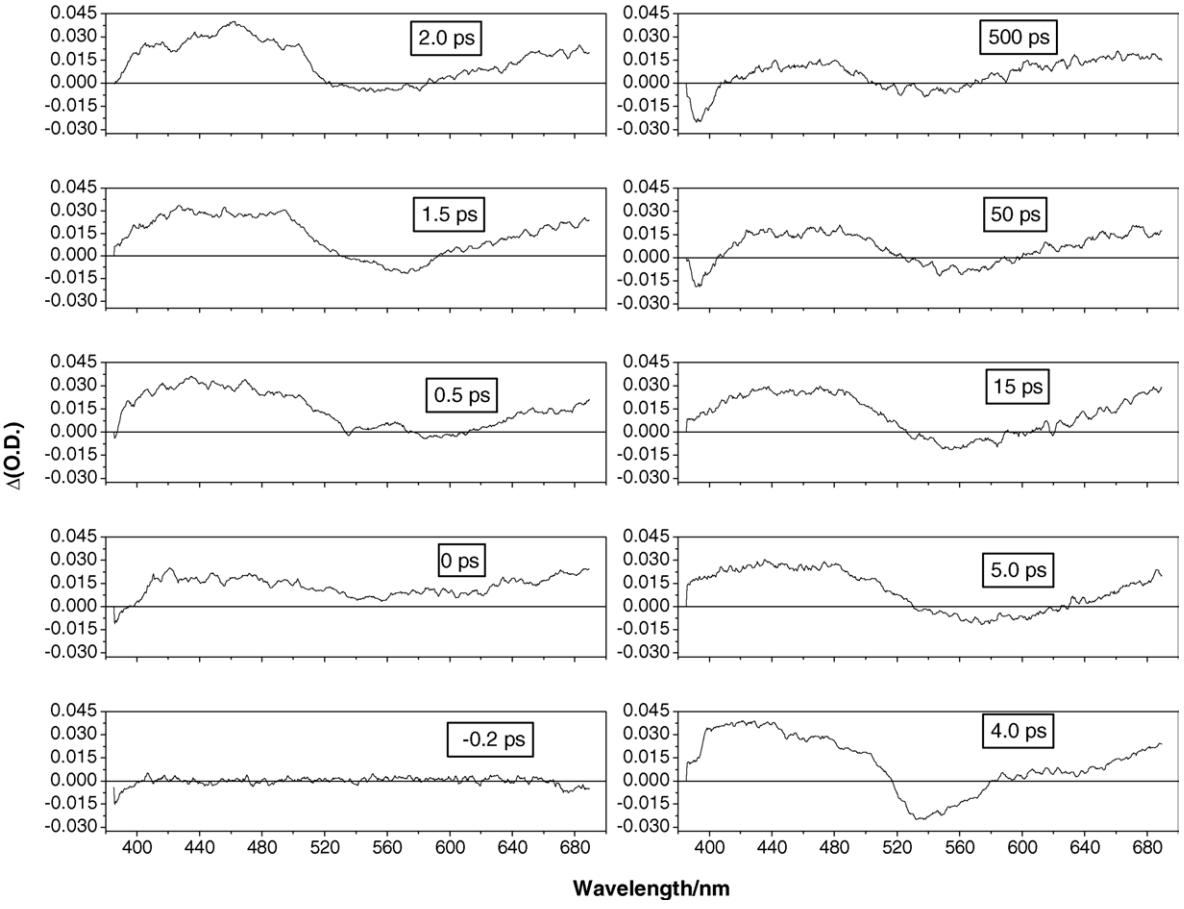

Fig. 3. Variation of transient absorption spectra of MFOH (**I**) in cyclohexane at different time delay of the 360 nm pump and supercontinuum probe pulse.

(DNBP) [45]. Ultrafast ESIPT from this initially excited enol structure causes a band at 420–500 nm region after a few picoseconds from the proton transferred keto tautomer (**b**, Scheme 1). Stimulated emission appears in the form of negative transient absorption at around 560 nm, which is very close to the steady state fluorescence emission (∼535 nm) of the ESIPT product in these solvents. The change in spectral shape of the stimulated emission and transient absorption indicates that the presence of vibrational relaxation process after the proton transfer occurs. This prediction is supported by characterization of the stationary points for different conformers of MFOH (**I**) by semi-empirical calculation reported previously [46] that showed that the adiabatic ESIPT from the enol tautomer (**a**) results about ∼5000 cm^{-1} excess vibrational energy in the $S_1(\pi\pi^*)$ surface of the keto form (**b**). Relaxation of the vibrationally "hot" proton transferred state to the vibrationally "cold" state at the minimum of the keto potential well is manifested by the change in spectral shape of the transient absorption and/or stimulated emission (Fig. 4). The presence of vibration relaxation after initial ESIPT is also confirmed by the time domain measurements of transient absorption described below.

Although time evolution of transient absorption spectra does not provide any straight forward evidence for the ESIPT phenomena considering the similar spectral position of the $S_n \leftarrow S_1$ absorption of the excited enol and keto tautomer, assignment of the new band at 420–500 nm region to the proton transferred form is substantiated while considering the following points. The intensity of transient absorption in this wavelength range grows upto few picoseconds and then starts decaying in nanosecond time range. In a typical adiabatic ESIPT cycle, the only growing step in the excited state is the formation of keto tautomer (**b**) from the initially excited state of enol structure, **a**. Also the appearance of stimulated emission around the same time range in the similar spectral position as observed for **I** and **II** in steady state fluorescence measurements indicates the formation of ESIPT tautomer.

To understand the dynamics of the ESIPT, the change in transient absorption with time was measured at the maxima of $S_n \leftarrow S_1$ absorption of tautomer (460 nm). The time domain absorption profiles could be reproduced well by fitting the experimental points with a sum of three exponential (one rise and two decay) functions Eq. (2) as judged by the statistical parameters like reduced chi-square (χ^2_R) and visual inspection of the distribution of weighted residuals.

$$A(t) = \sum_{i=0}^{2} a_i \exp\left(-\frac{t}{\tau_i}\right) \quad (2)$$

One of the representative decay curves is shown in Fig. 5 and Table 2 displays all the fitting parameters for **I** and **II** in different solvents. The measurements were done in two different time windows (8 ps and 50 ps) to isolate different decay components with precision. The ultrafast rise component was obtained from the smaller time window measurement and it was kept constant in the longer time window data to isolate the intermediate decay. The longest time component in these fitting procedure (τ_3, Table 2) was always kept constant to the fluorescence decay time measured by time correlated single photon counting (TCSPC) technique. All the measurements show a ultrafast rise component of ∼200 fs (for **I**) and

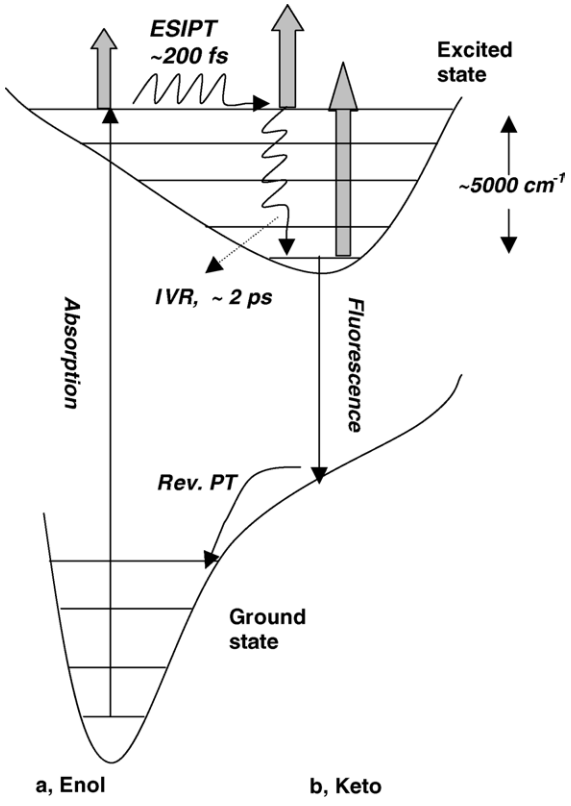

Fig. 4. Schematic view of ESIPT phenomena and corresponding time parameters for the compounds studied. Shaded block arrows indicate transient absorption at different time delay after excitation.

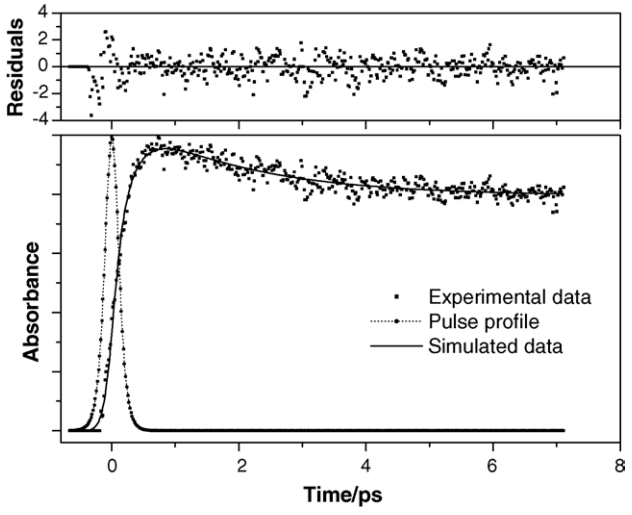

Fig. 5. Kinetics of transient absorption measured at 460 nm for MAOH (**II**) in chloroform. The distribution of weighted residuals is shown in the upper panel.

Table 2
Fitted parameters for the kinetic data measured at 460 nm transient absorption of **I** and **II** in different solvents[a]

System	Solvent	τ_1 (fs) (a_1)	τ_2 (ps) (a_2)	τ_3 (ns)[b] (a_3)
MFOH (**I**)	Cyclohexane	180 (−0.9)	2.7 (0.64)	1.2 (0.36)
	Chloroform	225 (−0.85)	2.9 (0.55)	1.3 (0.45)
MAOH (**II**)	Cyclohexane	250 (−0.9)	1.90 (0.30)	0.9 (0.7)
	Chloroform	300 (−1.0)	1.25 (0.32)	0.7 (0.68)

[a] Values in parenthesis are the pre-exponential factors associated with each decay time.
[b] Decay times kept fixed during the fitting procedure as obtained from time resolved fluorescence measurements (see text for details).

∼250 fs (for **II**) corresponding to the rate of intramolecular proton transfer. Recently, femtosecond time-resolved measurement on the ESIPT of 1-hydroxyanthraquinone (1-HAQ) in toluene reported similar time constant for proton transfer (∼260 fs) [47]. However, in a more recent paper, the same group measured the ESIPT dynamics of 1-HAQ to be about 120 fs with fluorescence up-conversion technique using two photon excitation [48]. They discussed the mechanism of ESIPT of 1-HAQ in the same line to that reported previously for 1,8-dihydroxyanthraquinone by Arzhantsev et al. [49]. The unique ESIPT mechanism in these anthraquinone derivatives involve the collapse of initially excited Franck-Condon state to a delocalized state which encompass both the keto and enol eigenstates in the S_1 potential energy surface with few tens to hundreds of femtoseconds. Also, as no significant difference in the ESIPT dynamics is observed with isotopic substitution [47] and almost instantaneous appearance of tautomer-type fluorescence [49] led them conclude a barrierless proton transfer mechanism in these systems.

In a previous paper, we have reported the construction of potential energy surface (PES) for ESIPT in MFOH theoretically [46]. Estimation of different vibrational levels and the corresponding eigenfunctions supported at the ground and excited PESs using the Fourier-Grid Hamiltonian (FGH) method showed that Franck-Condon excitation from the S_0 state would take the system *almost* over the barrier and eventually into the potential well representing the tautomeric (**b**) form. However, proton transfer from the enol (**a**) potential well to keto (**b**) form by tunneling could not be overruled completely and FGH-based complex coordinate rotation calculation estimates a tunneling rate constant of $\sim 10^{11}\ s^{-1}$. The measured ESIPT rate is faster by an order of magnitude and indicates the importance of over-barrier transfer in the S_1 surface. However, it is important to note here that the measured ESIPT times reported here are substantially slower than ESIPT in 3-HF reported recently [29]. In 3-HF, ESIPT occurs through a five-membered hydrogen bonded ring in contrast to a six-membered chelate ring in the present systems. So, it can be presumed that the geometry of the hydrogen bonded ring has a substantial effect on the rate of proton transfer. Recent high level ab-initio calculations have indeed confirmed this prediction [50,51]. In some of their elegant works [22,52], Riedle and coworkers analyzed the role of skeletal vibrations in the ESIPT reaction of HBT. It was shown that the proton transfer initiates with hydrogen chelate ring contraction by in-plane bending of the whole molecule and the new equilibrium of proton transferred geometry results at a critically shortened non-bonded O···N distance. In view of the above results, it can be argued that significantly slower rate of proton transfer in the investigated systems make them unique and the presence of a barrier in the proton transfer pathway indicates the probability of ESIPT to be less than unity for each individual skeletal approach. The time domain measurements corresponding to stimulated emission (560 nm) results only a single exponential decay in both the cases of **I** and **II**, which is very close to the respective fluorescence decay time of the keto tautomer (**b**). The rise part corresponding to ESIPT could not be detected at this wavelength due to very poor signal to noise ratio of the transient signal.

The 'relatively' slow proton transfer in these systems can further be justified by looking at the appearance of stimulated emission in Fig. 3. The stimulated emission in the transient absorption spectra for these systems is originated due to the formation of keto tautomer (**b**) resulting after ESIPT. In Fig. 3, it is seen that there is no trace of stimulated emission even in the time delay of 0.5 ps between the pump and probe pulse indicating the ESIPT as a *relatively slow process*.

The intermediate time component of few picoseconds (Table 2) in both the compounds ascribed due to the vibrational relaxation process of the hot proton transferred keto tautomer (**b**) which is also manifested by change in transient absorption spectral shape (discussed before). The time evolution of transient absorption spectra may be originated due to several reasons. Among these, the following three are mostly important (a) decay originated from the internal conversion (IC) of the higher excited electronic state, (b) cooling process of the vibrationally unrelaxed state through intramolecular vibrational redistribution (IVR), and (c) excess energy transfer to the surrounding solvent medium through an intermolecular mechanism. Both of the first two processes are known to occur within a few picoseconds for large organic molecules in solution, whereas, the last phenomenon occurs with a relatively longer time scale (ca. 5–50 ps), depending on the solvent and the excess vibrational energy [53,54]. However, for the ESIPT systems like **I** and **II**, we can neglect the first possibility because the proton transfer occurs from the first excited enol form to the keto form (S_1 and S_1', respectively in Fig. 4). So, the time dependent transient absorption spectral change during early time delay may be regarded as due to the intramolecular vibrational redistribution (IVR) of the hot proton transferred keto tautomer towards the formation of vibrationally cold state. Similar IVR process has also been reported recently for other ESIPT systems like 2-(2′-hydroxyphenyl)benzothiazole (HBT) [55] and hydroxyanthraquinone derivatives [47–49]. In large molecules like **I** and **II** in solution, the density of vibronic states is very high and the dissipation of excess vibrational energy within few picoseconds is understandable.

4. Conclusion

Excited state intramolecular proton transfer of MFOH (**I**) and its derivative, MAOH (**II**) have been studied in femtosecond to nanosecond timescale by femtosecond transient absorption and time resolved fluorescence measurements. Ultrafast ESIPT occurs at about ∼200 fs in **I** followed by an IVR component of about 2.8 ps before undergoing fluorescence decay from the excited state of proton transferred keto structure. The corresponding time constants for **II** are in the range of ∼250 fs and 1.5 ps, respectively. The relatively longer ESIPT time constant in these six membered hydrogen bonded chelate systems compared to the reported corresponding five membered analogue, 3-hydroxy flavone (3HF), is ascribed due to the necessity of large skeletal motion during the proton transfer process.

Acknowledgement

S. Mitra thanks Japan Society for Promotion of Science (JSPS) for supporting his stay at Kwansei Gakuin University as an invited fellow (L-03554).

References

[1] T. Bountis (Ed.), Proton Transfer in Hydrogen Bonded Systems, Plenum, New York, 1992.
[2] H.-H. Limbach, J. Manz (Eds.), Hydrogen Transfer: Experiment and Theory, Ber. Bunsenges. Phys. Chem. 102 (1998) 3523 (special issue).
[3] S. Scheiner, Hydrogen Bonding: A Theoretical Perspective, Oxford University Press, New York, 1997.
[4] E. Caldin, V. Gold (Eds.), Proton Transfer Reactions, Halsted Press, New York, 1975.
[5] For a recent review on biologically relevant excited state double proton transfer process see: P.T. Chou, J. Chin. Chem. Soc. 48 (2001) 651.
[6] T. Warner, G. Woessner, H.E. Kramer, in: S.P. Pappas, F.H. Winslow (Eds.), Photodegradation and Photostabilization of Coatings, vol. 151, ACS, Washington, DC, 1981, p. 1.
[7] P.T. Chou, D. McMorrow, T.J. Aartsma, M. Kasha, J. Phys. Chem. 88 (1984) 4596.
[8] M. Scherl, D. Harrer, J. Fischer, A. DeCian, J.-L. Lehn, Y. Eichen, J. Phys. Chem. 100 (1996) 16175.
[9] A. Sytnik, I. Litvinyuk, Proc. Natl. Acad. Sci. 93 (1996) 12959.
[10] R. Das, S. Mitra, D. Nath, S. Mukherjee, J. Phys. Chem. 100 (1996) 14514.
[11] S. Mitra, R. Das, S. Mukherjee, J. Phys. Chem. B 102 (1998) 3730.
[12] A. Douhal, J. Dabrio, R. Sastre, J. Phys. Chem. 100 (1996) 149.
[13] P.F. Barbara, H.P. Trommsdorf (Eds.), Chem. Phys. 136 (1989) 153 (special issue in proton transfer).
[14] M. Kasha Fetschrift, J. Phys. Chem. 95 (1991) 10215.
[15] S. Lochbrunner, K. Stock, V. De Waele, E. Riedle, in: A. Douhal, J. Santamaria (Eds.), Femtochemistry and Femtobiology; Ultrafast dynamics in molecular science, World Scientific, River Edge, NJ, 2002, p. 202.
[16] T. Arthen-Engeland, T. Bultmann, N.P. Ernsting, M.A. Rodriguez, W. Thiel, Chem. Phys. 163 (1992) 43.
[17] S. Lochbrunner, T. Schultz, M. Schmitt, J.P. Shaffer, M.Z. Zgierski, A. Stolow, J. Chem. Phys. 114 (2001) 2519.
[18] (a) F. Lärmer, T. Elsaesser, W. Kaiser, Chem. Phys. Lett. 148 (1988) 119–124;
(b) T. Elsaesser, F. Lärmer, W. Frey, Inst. Phys. Conf. Ser. 126 (1991) 543–545.
[19] C. Chudoba, E. Riedle, M. Pfeiffer, T. Elsaesser, Chem. Phys. Lett. 263 (1996) 622.
[20] D. Marks, H. Zhang, M. Glasbeek, J. Lumin. 76–77 (1998) 52–55.
[21] F.V.R. Neuwahl, P. Foggi, R.G. Brown, Chem. Phys. Lett. 319 (2000) 157.
[22] S. Lochbrunner, A.J. Wurzer, E. Riedle, J. Phys. Chem. A 107 (2003) 10580.
[23] N.P. Ernsting, S.A. Kovalenko, T. Senyushkina, J. Saam, V. Farztdinov, J. Phys. Chem. A 105 (2001) 3443.
[24] S. Takeuchi, T. Tahara, Chem. Phys. Lett. 347 (2001) 108–114;
S. Takeuchi, T. Tahara, J. Phys. Chem. A 102 (1998) 7740.
[25] D.E. Folmer, L. Poth, E.S. Wisniewski, A.W. Castleman Jr., Chem. Phys. Lett. 287 (1998) 1.
[26] T. Fiebig, M. Chachisvilis, M. Manger, A.H. Zewail, A. Douhal, I. Gracia-Ochoa, A. deLa Hoz Ayuso, J. Phys. Chem. A 103 (1999) 7419.
[27] J.L. Herek, S. Pederson, L. Benares, A.H. Zewail, J. Chem. Phys. 97 (1992) 9046.
[28] N.P. Ernsting, B. Dick, Chem. Phys. 136 (1989) 181.
[29] S. Ameer-Beg, S.M. Ormson, R.G. Brown, P. Matousek, M. Towrie, E.T.J. Nibbering, P. Foggi, F.V.R. Neuwahl, J. Phys. Chem. A 105 (2001) 3709.
[30] S. Mitra, R. Das, S. Mukherjee, Chem. Phys. Lett. 202 (1993) 549.
[31] S. Mitra, R. Das, S. Mukherjee, Chem. Phys. Lett. 228 (1994) 393.
[32] S.K. Mandal, K. Nag, J. Chem. Soc. Dalton Trans. (1984) 2141.
[33] S.K. Mandal, K. Nag, J. Org. Chem. 51 (1986) 3900.
[34] W.H. Melhuish, J. Phys. Chem. 65 (1961) 229.
[35] S. Mitra, N. Tamai, Chem. Phys. 246 (1999) 463.
[36] S. Mitra, N. Tamai, Phys. Chem. Chem. Phys. 5 (2003) 4647.
[37] N. Tamai, T. Asahi, H. Masuhara, Rev. Sci. Instrum. 64 (1993) 2496.
[38] M.A. Morgan, E. Orton, G.C. Pimentel, J. Phys. Chem. 94 (1990) 7927.
[39] S. Nagaoka, N. Hirota, M. Sumitani, K. Yoshihara, J. Am. Chem. Soc. 105 (1983) 4220.
[40] D.V. O'Connor, D. Philips, Time Correlated Single Photon Counting, Academic Press, London, 1984.
[41] P.M. Felker, W.R. Lambert, A.H. Zewail, J. Chem. Phys. 77 (1982) 1603.
[42] L.A. Heimbrook, J.E. Kenny, B.E. Kohler, G.W. Scott, J. Phys. Chem. 87 (1983) 280.
[43] S. Mitra, Ph.D Thesis, Jadavpur University, 1996.
[44] S. Mitra, N. Tamai, Chem. Phys. Lett. 282 (1998) 391.
[45] S. Mitra, H. Ito, N. Tamai, Chem. Phys. 306 (2004) 185–189.
[46] S. Mitra, R. Das, S.P. Bhattacharyya, S. Mukherjee, J. Phys. Chem. A 101 (1997) 293.
[47] J.R. Choi, S.C. Jeoung, D.W. Cho, Bull. Korean Chem. Soc. 24 (2003) 1675.
[48] J.R. Choi, S.C. Jeoung, D.W. Cho, Chem. Phys. Lett. 385 (2004) 384.
[49] S.Y. Arzhentsev, S. Takeuchi, T. Tahara, Chem. Phys. Lett. 330 (2000) 83.
[50] A.L. Sobolewski, W. Domcke, in: D. Heidrich (Ed.), The Reaction Path in Chemistry: Current Approaches and Perspectives, Kluwer Academic Publishers, Dordrecht, The Netherlands, 1995, p. 257.
[51] S. Schiener, J. Phys. Chem. A 104 (2000) 5898.
[52] R. De Vivie-Riedle, V.D. Waele, L. Kurtz, E. Riedle, J. Phys. Chem. A 107 (2003) 10591.
[53] A. Seilmeier, W. Kaiser, in: W. Kaiser (Ed.), Ultrashort Laser Pulses and Applications: Topics in Applied Physics, vol. 60, Springer, 1988 (Chapter 7).
[54] T. Fujino, T. Tahara, J. Phys. Chem. A 104 (2000) 4203.
[55] M. Rini, J. Dreyer, E.T.J. Nibbering, T. Elsaesser, Chem. Phys. Lett. 374 (2003) 13.